Available online at www.sciencedirect.com
SCIENCE DIRECT®
Journal of Organometallic Chemistry 690 (2005) 4945–4958
Journal of Organometallic Chemistry
www.elsevier.com/locate/jorganchem

New bromo-, triflato-, and hydridotricarbonylrhenium(I) complexes with diphosphinite ligands: Structural, spectral and protonation studies of various hydrides

Sandra Bolaño, Jorge Bravo *, Jesús Castro, Soledad García-Fontán *, M[a] Carmen Marín, Pilar Rodríguez-Seoane

Departamento de Química Inorgánica, Universidade de Vigo, Lagoas-Marcosende, E-36310 Vigo, Spain

Received 23 May 2005; received in revised form 29 July 2005; accepted 4 August 2005
Available online 22 September 2005

Abstract

Bromotricarbonylrhenium(I) complexes [$ReBr(CO)_3L$] [$L = Ph_2PO(CH_2)_3OPPh_2$ ($\mathbf{L^1}$), $^iPr_2PO(CH_2)_2OP^iPr_2$ ($\mathbf{L^2}$), $Cy_2PO(CH_2)_2OPCy_2$ ($\mathbf{L^3}$)] were prepared by reaction of [$ReBr(CO)_5$] with L. X-ray crystallography showed them all to be mononuclear, with the CO ligands *fac*. Subsequent reaction with AgOTf gave *fac*-[$Re(OTf)(CO)_3L$], as shown by IR and NMR spectra. By contrast, reaction of [$ReH(CO)_5$] with $\mathbf{L^{1-3}}$ gave hydrido complexes, the nuclearity and stereochemistry of which depended on the identity of L, as was confirmed by X-ray crystallography of *mer*-[$ReH(CO)_3\mathbf{L^1}$], *fac*-[$ReH(CO)_3\mathbf{L^2}$] and [$\{ReH(CO)_4\}_2(\mu\text{-}\mathbf{L^3})$]. Protonation of the hydrido compounds at 183 K with $HBF_4 \cdot OMe_2$ gave the corresponding non-classical cationic dihydrogen complexes ($T_{1(min)} \sim 15$ ms at 400 MHz), which released H_2 at temperatures above critical temperatures (243–263 K) that depended on the co-ligands.

Keywords: Rhenium; Carbonyl; Triflato; Hydrido compounds; Dihydrogen compounds; Phosphinites

1. Introduction

Transition metal hydrido compounds can be used as efficient catalysts for homogeneous processes [1] and as new materials for storage of hydrogen [2]. Phosphines can be readily employed in such complexes as supporting ligands due to their easily modified electronic and steric effects allow modulation of catalytic behaviour. Moreover, the use of potential chelating ligands offers extra control over the selectivity of many catalytic reactions [3].

The field of organorhenium chemistry has progressed significantly in recent decades [4], and a large number of rhenium hydrido complexes bearing phosphines as co-ligands are known. However, few that bear phosphinites have been used [5]. The weaker σ-donor and stronger π-acceptor nature of phosphinites [6] may be expected to influence the properties of the metal centre, and hence those of the complex.

We have previously investigated the properties and fluxional behaviour of a number of halide and hydrido rhenium complexes bearing mono- and bidentate phosphinites, phosphonites or phosphites, finding significant dependence on the nature of the phosphorus-bearing ligands [7]. In this paper, we report the synthesis and properties of hydrido-, bromo- and triflatorhenium(I) carbonyl complexes with three diphosphinite ligands differing in the nature of the R groups bound to the P atom and in the length (two or three carbons) of the alkyl chain linking the two R_2PO groups.

* Corresponding authors. Tel.: +34 986812275; fax: +34 986813798.
E-mail addresses: jbravo@uvigo.es (J. Bravo), sgarcia@uvigo.es (S. García-Fontán).

0022-328X/$ - see front matter © 2005 Elsevier B.V. All rights reserved.
doi:10.1016/j.jorganchem.2005.08.014

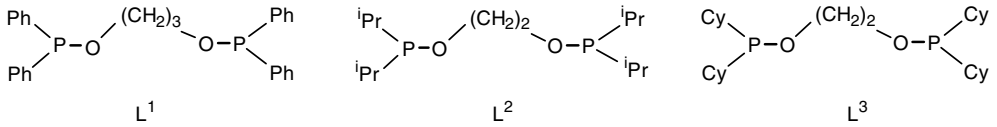

Scheme 1. Diphosphinite ligands $\mathbf{L^{1-3}}$.

2. Results and discussion

2.1. Diphosphinite ligands

The new diphosphinite ligand 1,3-bis(diphenylphosphinoxy)propane ($\mathbf{L^1}$) and the known ligands 1,2-bis(diisopropylphosphinoxy)ethane ($\mathbf{L^2}$) and 1,2-bis(dicyclohexylphosphinoxy)ethane ($\mathbf{L^3}$) (Scheme 1) were prepared following a previously published method [8] by reaction of the corresponding diol with a chlorophosphine in the presence of triethylamine. As expected, their $^{31}P\{^1H\}$ NMR spectra in $CDCl_3$ show just a single signal for the two phosphorus atoms ($\mathbf{L^1}$, δ 112.6; $\mathbf{L^2}$, δ 154.9; $\mathbf{L^3}$, δ 150.1 ppm).

2.2. Bromotricarbonylrhenium(I) complexes

2.2.1. Synthesis and spectroscopic characterization

Reaction of ligands $\mathbf{L^{1-3}}$ with $[ReBr(CO)_5]$ in 1:1 mole ratio in refluxing toluene replaced two CO ligands with the corresponding bidentate ligand, affording the new bromotricarbonyl complexes *fac*-$[ReBr(CO)_3L]$ (**1a–c**; Scheme 2).

The new complexes are stable in the solid state and in solution at room temperature, and were characterized by the usual spectroscopic techniques. In their IR spectra, three strong ν(CO) bands characteristic of the *fac*-$Re^I(CO)_3$ moiety are observed at 2031, 1948 and 1922 cm^{-1} for **1a**, 2029, 1951 and 1897 cm^{-1} for **1b**, and 2022, 1954 and 1888 cm^{-1} for **1c** [9]. The $^{31}P\{^1H\}$ NMR spectra of complexes **1a–c** show single resonances (showing the magnetic equivalence of the two phosphorus nuclei), with negative coordination shifts in all cases. In keeping with the *fac* arrangement of the CO ligands, the $^{13}C\{^1H\}$ NMR spectra show two low-field signals assignable to the CO groups: a triplet corresponding to the CO group located *cis* to both phosphorus nuclei ($\delta \sim 189$ ppm; $^2J_{CP} \sim 7$ Hz), and a multiplet ($\delta \sim 188$ ppm) corresponding to the other two CO ligands.

2.2.2. Description of the structures

Perspective views of the molecular structures of compounds **1a–c** with atom numbering scheme are shown in Figs. 1–3, respectively. Selected bond lengths and bond angles are listed in Table 1, while the crystallographic data and the details of the structure determination are given in Table 4.

X-ray crystallography showed that **1a–c** all consist of discrete molecules with no significant hydrogen bonds between neighbours. In each complex, the central rhenium atom is surrounded by three facially arranged carbonyl ligands, one bromine atom, and the two phosphorus atoms of the bidentate ligand L (Figs. 1–3). The Re–C distances of the carbonyl ligands *trans* to the phosphorus atoms range from 1.931(7) to 1.967(8) Å, while that of the CO *trans* to the bromine atom is significantly shorter due to the π-donor character of the Br which increases the Re–CO backbonding. However, all the Re–X bond lengths (X = C, Br, P) are in the ranges found among similar complexes [7d,10]. The angles around the metal are close to those of a regular octahedron; the greatest distortion is present in compound **1b**, in which, probably due to the steric hindrance of the isopropyl groups, the *cis* angles range from 85.7(2)° to 94.89(5)° and the narrowest axial angle is 172.43(17)°.

In compound **1a** the conformation of the eight-membered chelate ring can be described as a chair [11], the planes defined by {Re, P(1), P(2), O(51), O(52)} and {C(51), C(52), C(53)} being almost parallel [dihedral angle 2.8(3)°]. The seven-membered chelate rings of compounds **1b** and **1c** are both best described as a boat with an intramolecular interaction between the bromine atom and a methylene proton belonging to the bidentate ligand (H–Br = 2.84 Å in **1b** and 2.59 Å in **1c**).

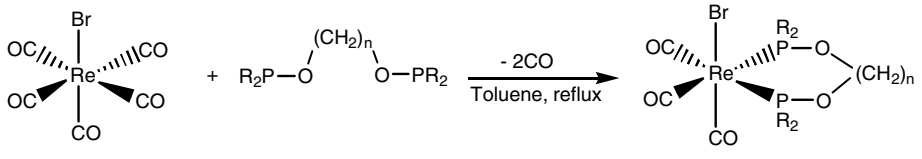

1a: R= Ph ; n = 3
1b: R= ^{i}Pr ; n = 2
1c: R= Cy ; n = 2

Scheme 2. Synthesis of the complexes **1a–c**.

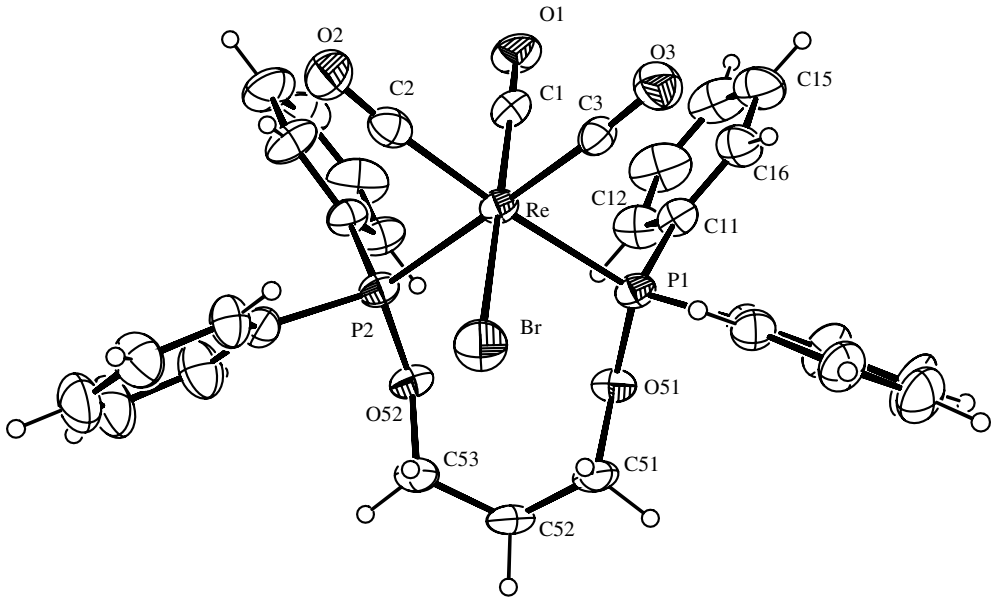

Fig. 1. Molecular structure of **1a**.

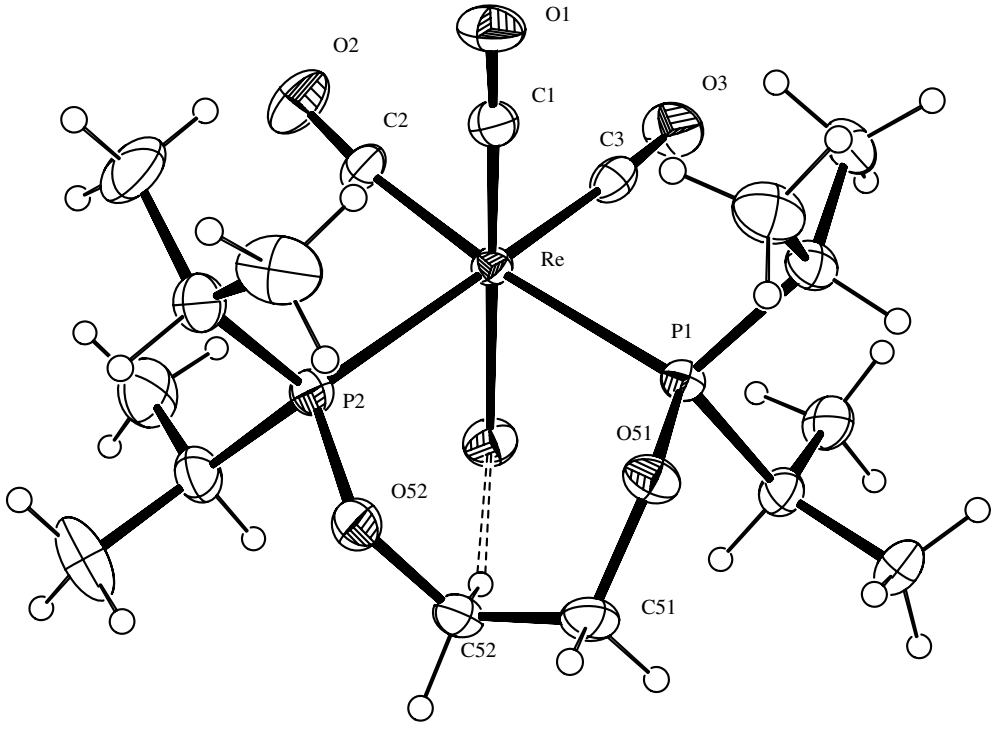

Fig. 2. Molecular structure of **1b.**

2.3. Triflatotricarbonylrhenium(I) complexes

When compounds **1a**–**c** were reacted with $Ag(SO_3CF_3)$ in 1:1 mole ratio in refluxing CH_2Cl_2, the corresponding triflato derivatives were obtained through replacement of the bromo ligand by OTf (Scheme 3).

Complexes **2a**–**c** were stable in the solid state and in methylene chloride solution at room temperature, and their IR spectra all showed three strong bands in the region 1914–2042 cm^{-1} that can be assigned to the CO stretching vibrations. These bands are blue-shifted by about 17 cm^{-1} with respect to those of complexes **1a**–**c**, which is attributable to OTf having greater electron-withdrawing power than Br. $^{31}P\{^1H\}$ and $^{13}C\{^1H\}$ NMR spectra of complexes **2a**–**c** showed that the *fac* arrangement of the CO groups is inherited from the Br compounds: the $^{31}P\{^1H\}$ NMR

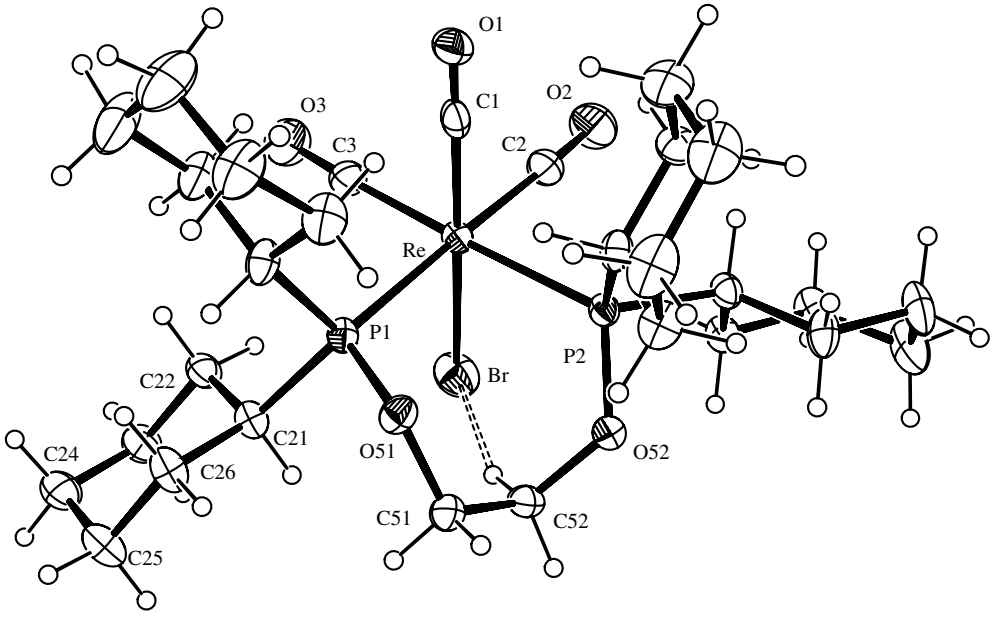

Fig. 3. Molecular structure of **1c**.

Table 1
Selected bond lengths (Å) and angles (°) in the bromo complexes

Complex	**1a**	**1b**	**1c**
Bond lengths (Å)			
Re–C(1)	1.919(7)	1.889(6)	1.931(8)
Re–C(2)	1.967(8)	1.938(7)	1.950(7)
Re–C(3)	1.931(7)	1.956(6)	1.958(7)
Re–P(1)	2.474(2)	2.495(2)	2.474(2)
Re–P(2)	2.462(2)	2.467(1)	2.479(2)
Re–Br	2.621(1)	2.632(1)	2.654(1)
Bond angles (°)			
C(1)–Re–C(2)	88.4(3)	86.3(3)	88.5(3)
C(1)–Re–C(3)	89.3(3)	92.7(2)	86.9(3)
C(1)–Re–P(1)	88.3(2)	90.2(2)	92.2(2)
C(1)–Re–P(2)	90.5(2)	93.0(2)	90.8(2)
C(2)–Re–C(3)	90.6(3)	85.7(2)	89.1(3)
C(2)–Re–P(2)	88.6(2)	89.8(2)	90.7(2)
C(3)–Re–P(1)	87.3(2)	90.0(2)	92.6(2)
P(1)–Re–P(2)	93.4(1)	94.9(1)	87.7(1)
C(2)–Re–Br	90.4(2)	92.7(2)	86.9(2)
C(3)–Re–Br	89.6(2)	86.2(2)	88.1(2)
P(1)–Re–Br	92.9(1)	90.8(1)	92.5(1)
P(2)–Re–Br	90.5(1)	88.0(1)	94.2(1)
C(3)–Re–P(2)	179.2(2)	172.4(2)	177.7(2)
C(1)–Re–Br	178.4(2)	178.6(2)	173.3(2)
C(2)–Re–P(1)	176.1(2)	174.3(2)	178.2(2)

spectra all showed a single singlet, and the $^{13}C\{^1H\}$ spectra two low-field signals of structure and multiplicity similar to those observed for the bromo derivatives.

2.4. Hydridotricarbonylrhenium(I) complexes

2.4.1. Synthesis and spectroscopic characterization of *mer*-[ReH(CO)$_3$**L**^{1}] (**3a**)

Reaction of [ReH(CO)$_5$] with **L**^{1} afforded *mer*-[ReH(CO)$_3$**L**^{1}] (**3a**) in 39% yield (Scheme 4). The crude reaction product was contaminated with about 1% of what, on the basis of ^{1}H and ^{31}P NMR data, was tentatively identified as the *fac* isomer **3a**′ [^{1}H (CD_2Cl_2): δ −4.76 ppm (t, $J_{PH} = 27$ Hz, ReH); $^{31}P\{^1H\}$ (CD_2Cl_2): δ 122.8 ppm (s)]. Washing with THF and subsequent recrystallization from 2:10 (v/v) CH_2Cl_2/EtOH solution afforded pure **3a**.

The IR spectrum of **3a** shows the CO vibrations as two strong bands at 1917 and 1954 cm^{-1} and a medium-strength band at 2035 cm^{-1}. The $^{31}P\{^1H\}$ NMR spectrum of **3a** shows the two doublets that are expected for two non-equivalent phosphorus nuclei (at 120.8 and 124.4 ppm; $J_{PP} = 23$ Hz), but its ^{1}H NMR spectrum surprisingly shows, at high field, only a single doublet for the hydrido

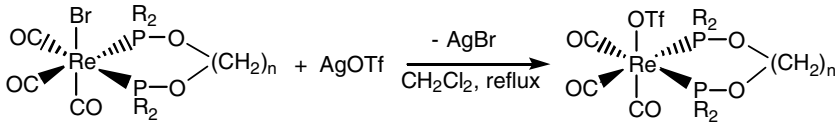

2a: R = Ph; n = 3
2b: R = ^{i}Pr; n = 2
2c: R = Cy; n = 2

Scheme 3. Synthesis of the complexes **2a**–**c**.

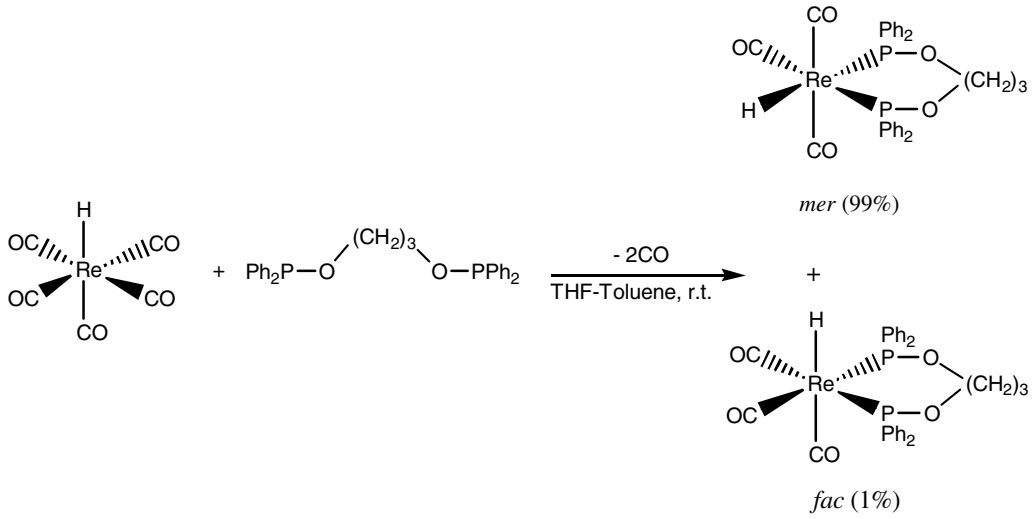

Scheme 4. Synthesis of the complex **3a**.

nucleus (δ −6.09 ppm; $J_{PH} = 36$ Hz), which suggests that coupling between the hydrido and one of the phosphorus nuclei must be almost zero. Two multiplets located at 2.02 ppm (2H) and 3.91 ppm (4H) may be assigned to the methylene protons of the diphosphinite ligand.

Lowering the temperature from 293 to 183 K just slightly broadens the $^{31}P\{^1H\}$ signals. In the ^1H NMR spectrum the hydrido doublet and the multiplet at 2.02 ppm are broadened more markedly, and the multiplet at 3.91 ppm decoalesces into three new broad signals, two of which integrate to 1 proton and one to 2. These changes appear to reflect the initial stages of the freezing of an equilibrium between conformers of the chelate ring, as has been observed in similar systems [7a]. Determination of the minimum spin-lattice relaxation time [$T_{1(min)}$] for the hydrido nucleus at 400 MHz by the standard inversion-recovery method gave a value of 296 ms at 215 K.

2.4.2. Synthesis and spectroscopic characterization of *fac*-[ReH(CO)$_3$**L**^{2}] (**3b**)

When [ReH(CO)$_5$] was reacted with **L**^{2} in 1:3 mole ratio in THF, chromatography of the crude product afforded *fac*-[ReH(CO)$_3$**L**^{2}] (**3b**; Scheme 5) [12].

The room-temperature ^1H NMR spectrum of **3b** displays a triplet at −5.69 ppm ($J_{HP} = 27$ Hz) that integrates to one proton corresponding to the hydrido ligand. The two multiplets at 2.16 and 2.32 ppm can be assigned to ^{i}Pr methine protons, and those at 4.03 and 4.23 ppm to the methylene protons of the chelate ring. The $^{31}P\{^1H\}$ NMR spectrum of **3b** shows a singlet at 149.5 ppm, indicating the magnetic equivalence of the two phosphorus nuclei at room temperature.

When the temperature was lowered from 293 to 173 K, the triplet observed at −5.69 ppm in the room-temperature ^1H NMR spectrum became a single broad signal, and the two multiplets corresponding to the methylene protons collapsed into a single broad hump (Fig. 4). In the $^{31}P\{^1H\}$ NMR spectrum of **3b** (Fig. 5) the signal observed at 293 K broadened progressively, disappeared into the baseline at 193 K, and re-emerged at 173 K as two broad signals at 132.6 and 167.1 ppm, indicating the magnetic non-equivalence of the two phosphorus nuclei at this temperature. $\Delta G^{\ddagger}$ was calculated as 31.35 ± 0.2 kJ mol^{-1} at the coalescence temperature, 193 K [13]. The fluxional process responsible for this behaviour is probably interconversion between two conformers of the seven-membered chelate ring [14]. Determination of $T_{1(min)}$ for the hydrido nucleus at 400 MHz by the standard inversion-recovery method gave a value of 234 ms at 190 K.

2.4.3. Synthesis and spectroscopic characterization of *fac*-[ReH(CO)$_3$**L**^{3}] (**3c**) and [{ReH(CO)$_4$}$_2$(μ-**L**^{3})] (**3c**′)

Reaction of [ReH(CO)$_5$] with ligand **L**^{3} in 1:3 mole ratio gave a 3:7 mixture of two products that were subsequently separated by column chromatography. The minor component was identified as the mononuclear compound

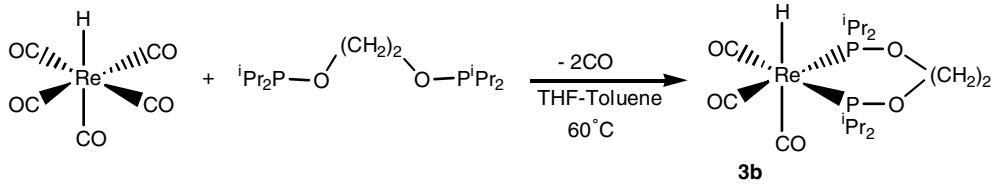

Scheme 5. Synthesis of the complex **3b**.

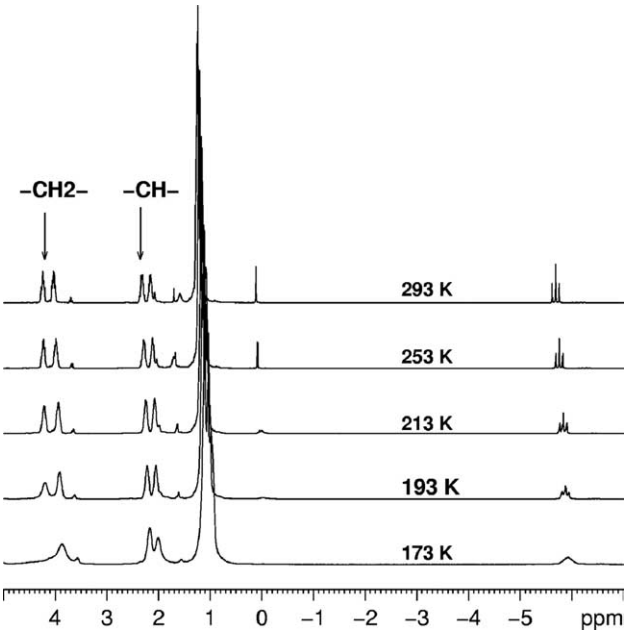

Fig. 4. ^{1}H NMR spectra of compound **3b** at various temperatures.

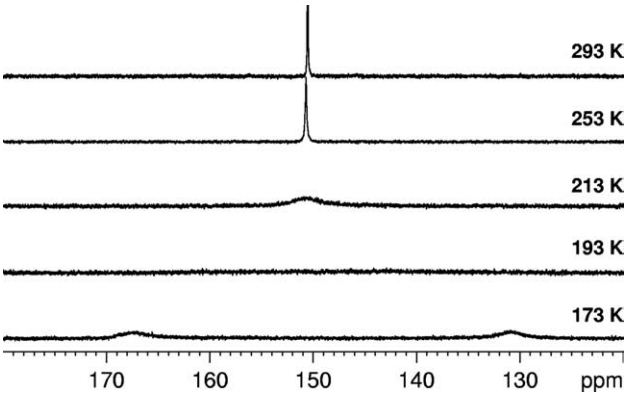

Fig. 5. ^{31}P{^{1}H} NMR spectra of compound **3b** at various temperatures.

fac-[ReH(CO)$_3$**L**^{3}] (**3c**), and the major component as the binuclear compound [{ReH(CO)$_4$}$_2$(μ-**L**^{3})] (**3c′**); see Scheme 6.

At 298 K, the ^{31}P{^{1}H} NMR spectrum of **3c** displays a singlet at 143.5 ppm and the ^{1}H NMR spectrum a triplet at −5.68 ppm ($J_{PH} = 27$ Hz). As in the case of similar systems [7], the signals corresponding to the methylene protons of the bidentate ligand appear as two multiplets (at 3.93 and 4.13 ppm), indicating their diastereotopic nature. The ^{13}C{^{1}H} spectrum shows, at low field, a triplet ($\delta =$ 196.0 ppm, $J_{CP} = 8$ Hz) and a multiplet ($\delta = 194.9$ ppm), the integrals of which are in an approximate ratio of 1:2. These results support the formulation of compound **3c** as the *fac* isomer of [ReH(CO)$_3$**L**^{3}]. Upon lowering the temperature to 173 K, the singlet at 143.5 ppm in the room-temperature ^{31}P{^{1}H} NMR spectrum broadens gradually until, at 203 K, it disappears into the baseline. The collapse of the methylene signals into a single broad signal at 193 K may be interpreted in the same way as for compound **3b**, i.e., as indicating the initial freezing of the interconversion between two conformers of the seven-membered chelate ring. The value of $T_{1(min)}$ found for the hydrido signal, 224 ms at 400 MHz.

The room-temperature ^{31}P{^{1}H} NMR spectrum of the major component of the mixture, **3c′**, shows a single singlet at 145.9 ppm, indicating the magnetic equivalence of the two phosphorus nuclei. In the ^{1}H NMR spectrum there is a doublet at high field ($\delta = -6.17$ ppm, $J_{HP} = 23$ Hz), and the appearance of the methylene proton signal as a single narrow multiplet (at 3.93 ppm) shows that in **3c′**, with its bridging ligand, the environment of these nuclei is more uniform than in **3c**, with its more restrictive chelating ligand. In agreement with these results, the ^{13}C{^{1}H} NMR spectrum shows, at low field, three doublets attributable to the CO groups: one at 190.5 ppm ($J_{CP} = 43$ Hz) corresponding to the CO *trans* to the P atom, one at 192.0 ppm ($J_{CP} = 10$ Hz) that is assignable to the mutually *trans* CO groups (this signal integrates to approximately double the previous one), and one at 192.2 ppm ($J_{CP} = 7$ Hz) corresponding to the CO *trans* to the H atom. When the temperature is lowered from 293 to 173 K, the signals of the ^{1}H and ^{31}P{^{1}H} spectra broaden just slightly, in keeping with the proposed formulation. The value of $T_{1(min)}$ for the hydrido signal at 400 MHz is 320 ms; this

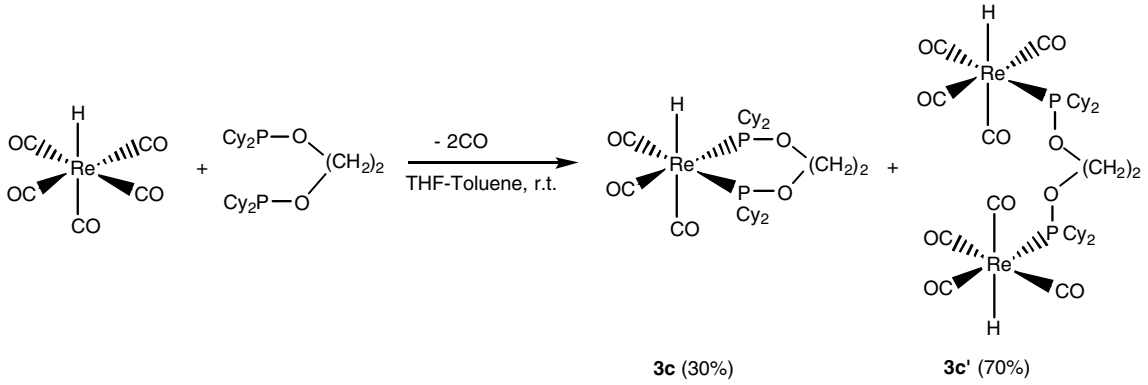

Scheme 6. Synthesis of the complexes **3c** and **3c′**.

value is significantly higher than that obtained for compound **3c**, possibly due to their having different numbers of P nuclei in the vicinity of the hydrido ligand [15].

2.4.4. Description of the structures

Perspective views of the molecular structures of compounds **3a**, **3b** and **3c′** with atom numbering scheme are shown in Figs. 6–8, respectively. Selected bond lengths and bond angles are listed in Table 2, while the crystallographic data and the details of the structure determination are given in Table 5.

X-ray crystallography confirmed the structures proposed for complexes **3a**, **3b** and **3c′** on the basis of their spectra, and showed them to consist of discrete molecules with no significant H-bonds between neighbours (Figs. 6–8). The apparent Re–H distances range from 1.60(5) to

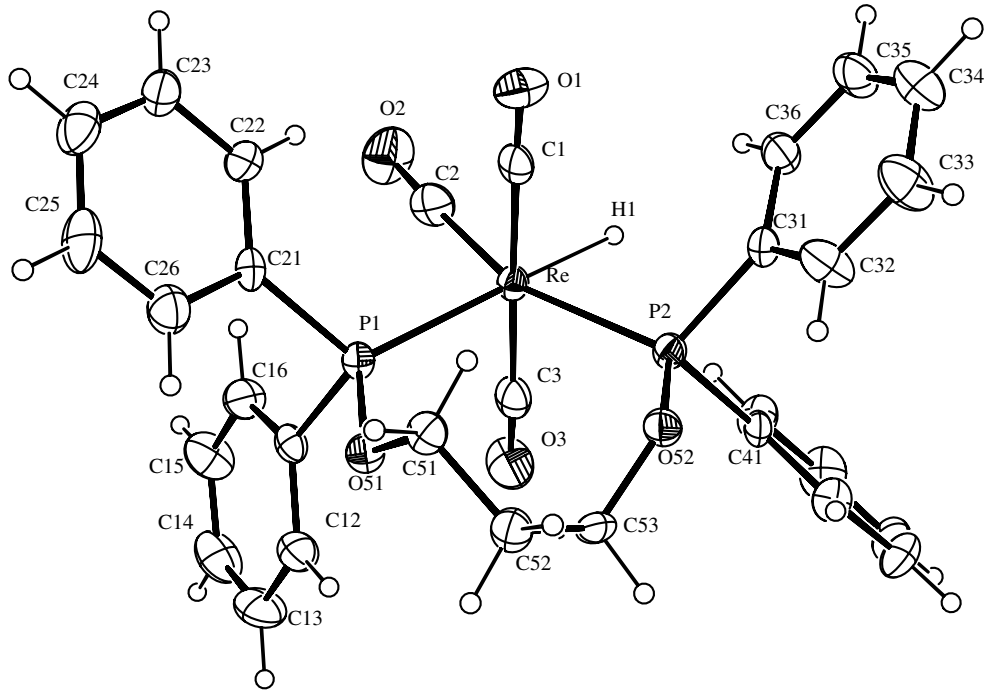

Fig. 6. Molecular structure of **3a**.

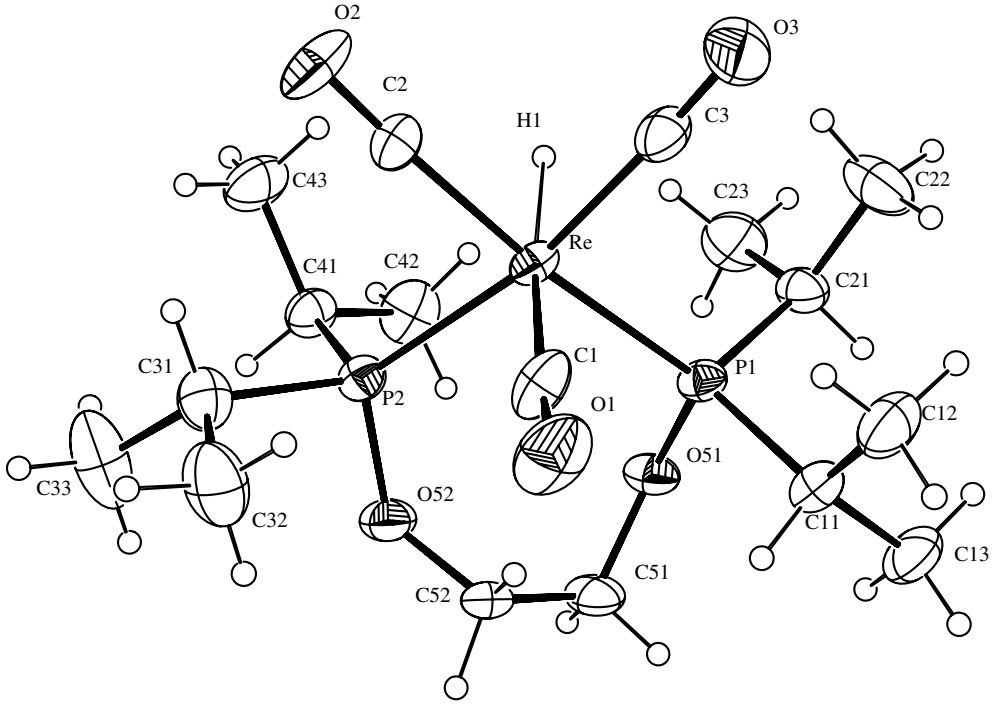

Fig. 7. Molecular structure of **3b**.

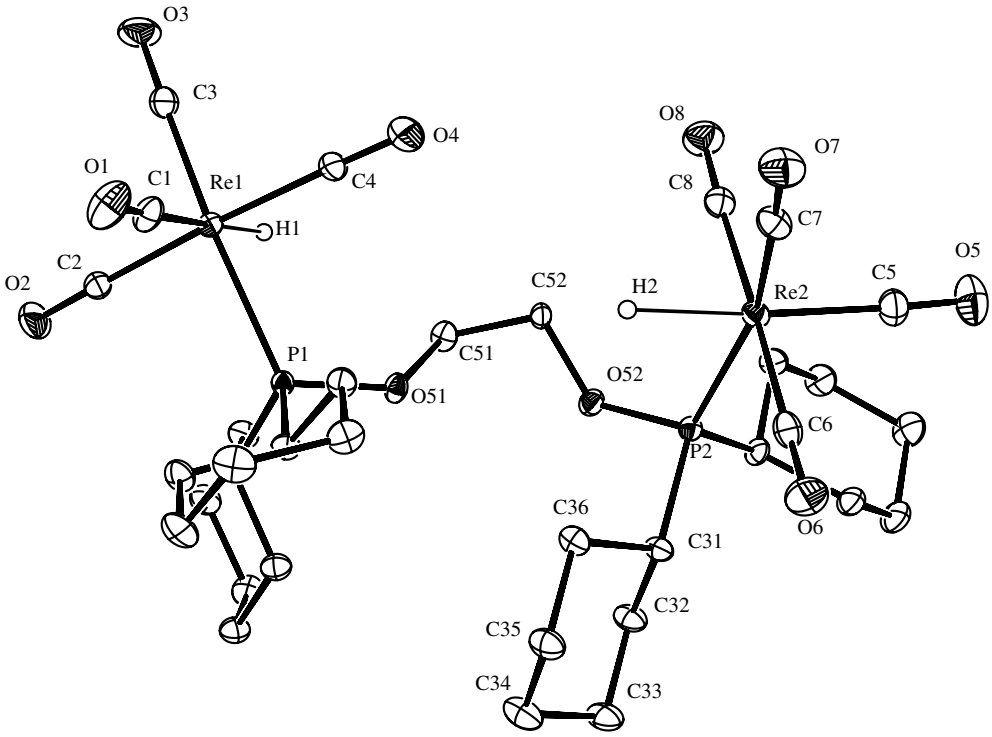

Fig. 8. Molecular structure of **3c′**.

1.90(4) Å, but these figures may be misleading due to the well-known limitations of X-ray diffractometry for hydrido ligands coordinated to third-row transition metals.

*2.4.4.1. Compound **3a**.* Complex **3a** is, to the best of our knowledge, the first mononuclear monohydrido complex with an $ReHP_2(CO)_3$ core to have been found by X-ray crystallography to have its hydrido ligand *trans* to the phosphorus atom. Among the different factors that could favour the formation of the *mer* stereoisomer, the large bite angle of $\mathbf{L^1}$ ligand could be a likely one. The coordination polyhedron is a distorted octahedron, the sources of the distortion being the small size of the hydrogen atom and the steric requirements of the bidentate ligand. Thus, the chelate angle is 107.3(5)°, and P(2) lies 0.81(1) Å from the plane defined by the three carbonyl ligands. The Re–P bond lengths are 2.385(2) and 2.405(1) Å, the shorter corresponding to the phosphorus atom *trans* to the hydrido ligand, which exerts less *trans* influence than the carbonyl ligand [16]. Both these distances are slightly shorter than those found in the similar complex *fac*-[$ReH(CO)_3P$], [P = 1,2-bis(diphenylphosphinoxy)ethane] [7d], in which the chelate ring is seven-membered, but they are slightly longer than those found in a *trans-mer* complex with monodentate phosphorus-donor ligands [16]. The three Re–C distances are in keeping with the expected *trans* influences: an average 1.926(7) Å for the mutually *trans* carbonyl ligands, and 1.901(6) for the carbonyl *trans* to a phosphorus atom. These distances are significantly shorter than those found in the related complexes mentioned above [16,7d], but are close to those found in [$ReH(CO)_2$(triphos)] [17]. The eight-membered ring has a twisted boat conformation with six atoms virtually coplanar (rms deviation of 0.063 Å), C(53) 0.816(6) Å above the plane, and C(51) 0.832(6) Å below it (Fig. 9).

*2.4.4.2. Compound **3b**.* In **3b** the Re–C(2) and Re–C(3) bond lengths are slightly shorter than Re–C(1) (Table 2), as expected from the π-donor capacity of the P atom that increases the Re–CO backbonding. The Re–P distances are both longer than those reported in the literature for mononuclear complexes [16,7d]. The angles around the metal are more distorted than in the bromo analogue, with *cis* angles ranging from 82.0(3) to 95.6(2)° and axial angles from 167.9 (2)° to 174.9(1)° (the latter for C–Re–H). The Re–ligand bonds in the equatorial plane are all bent towards the hydrido, so that the rhenium atom lies 0.182(2) Å from the best equatorial plane, on the opposite side from the hydrido atom. As in **1b**, the conformation of the seven-membered chelate ring of **3b** is best described as a boat, with O(51) 0.112 (4) Å below the best plane and the other C and O atoms above it [O(52) by 0.678 (4) Å, C(51) by 0.964 (6) Å, and C(52) by 1.595(5) Å].

*2.4.4.3. Compound **3c′**.* Low-temperature X-ray diffractometry of compound **3c′** confirmed that this complex is a binuclear compound in which both rhenium(I) atoms are surrounded by four carbonyl ligands, a hydrido ligand, and one of the phosphorus atoms of the bis-monodentate ligand that bridges between them. The coordination polyhedra are slightly distorted octahedra with similar bond lengths, except that all the distances around Re(1) are

Table 2
Selected bond lengths (Å) and angles (°) in the hydrido complexes

Complex	**3a**	**3b**	**3c′**	
			(**Re1**)	(**Re2**)
Bond lengths (Å)				
Re–H(1)	1.75(4)	1.90(4)	1.60(5)	1.86(5)
Re–C(1)	1.925(7)	1.967(6)	1.967(6)	1.983(6)
Re–C(2)	1.901(6)	1.943(5)	1.973(6)	1.990(6)
Re–C(3)	1.927(7)	1.929(6)	1.951(5)	1.954(6)
Re–P(1)	2.385(2)	2.439(1)	2.440(1)	2.443(1)
Re–P(2)	2.405(2)	2.438(2)		
Re–C(4)			1.987(6)	1.987(5)
Bond angles (°)				
H(1)–Re–C(1)	94.2(1)	174.9(1)	173.2(2)	176(2)
H(1)–Re–C(2)	82.7(1)	87.8(1)	88.5(1)	91(2)
H(1)–Re–C(3)	85.7(1)	82.0(1)	76.9(2)	86.4(2)
C(1)–Re–C(2)	90.5(3)	95.9(2)	91.8(2)	92.5(2)
C(2)–Re–C(3)	91.2(3)	86.0(2)	87.6(2)	89.7(2)
C(1)–Re–C(3)	178.2(3)	94.7(3)	96.3(3)	95.2(2)
H(1)–Re–P(1)	172.1(1)	83.1(1)	79.8(2)	86.9(2)
H(1)–Re–P(2)	77.5(1)	88.0(1)		
C(1)–Re–P(1)	92.4(2)	93.2(1)	98.7(1)	99.9(2)
C(2)–Re–P(1)	92.9(2)	170.8(2)	88.4(1)	88.7(2)
C(3)–Re–P(1)	87.9(2)	91.5(1)	166.0(2)	163.5(2)
C(1)–Re–P(2)	86.6(2)	95.6(2)		
C(2)–Re–P(2)	159.7(2)	86.8(1)		
C(3)–Re–P(2)	91.6(2)	167.9(2)		
P(1)–Re–P(2)	107.3(5)	94.1(4)		
H(1)–Re–C(4)			84(2)	88.5(1)
P(1)–Re–C(4)			89.2(1)	92.7(2)
C(1)–Re–C(4)			91.8(3)	91.0(2)
C(2)–Re–C(4)			175.4(2)	176.6(2)
C(3)–Re–C(4)			91.7(2)	90.2(2)

(**Re1**) Values corresponding to the environment of the rhenium atom labelled Re(1).
(**Re2**) Values corresponding to the environment of the rhenium atom labelled Re(2), with P(2) represented by P(1), H(2) by H(1), C(5) by C(1), C(6) by C(2), C(7) by C(3), and C(8) by C(4).

slightly longer than those around Re(2). Unlike those of the related mononuclear complex [ReH(CO)$_4${P-Ph$_2$(OMe)}] [16], in **3c′** the angles showing most deviation

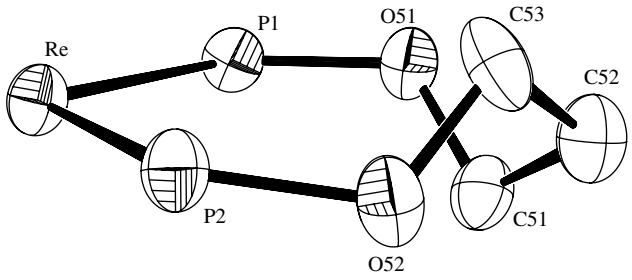

Fig. 9. Eight-membered ring in **3a**.

from their ideal values are the axial angles P–Re–C, 163.5(2)° and 166.0(2)°, probably due to the greater steric demands of the cyclohexyl substituents. If angles involving the hydrido ligand are ignored because of the unreliability of X-ray measurements of these angles, the most distorted *cis* angles are those between the phosphorus atom and the carbon *trans* to the hydrido ligand, with values of 98.7(1)° and 99.9(2)° around Re(1) and Re(2), respectively. The octahedra can thus be considered as fairly regular except for the position of the phosphorus atom, which has swung towards the hydrido ligand; as a result, the phosphorus atoms, instead of being in the same plane as three carbonyl carbon atoms, are 0.42(1) and 0.58(1) Å from the plane defined by those carbons, with the rhenium atoms on the other side of this plane and, respectively, 0.075(4) and 0.045(4) Å from it.

2.4.5. Protonation studies

Protonation of **3a**, **3b**, **3c** and **3c′** with $HBF_4 \cdot Me_2O$ in CD_2Cl_2 at 183 K gave the corresponding cationic dihydrogen complexes *mer*-[Re(η^2-H$_2$)(CO)$_3$**L^1**]$^+$(**3a***), *fac*-[Re(η^2-H$_2$)(CO)$_3$**L^2**]$^+$(**3b***), *fac*-[Re(η^2-H$_2$)(CO)$_3$**L^3**]$^+$ (**3c***) and [{Re(η^2-H$_2$)(CO)$_4$}$_2$(μ-**L^3**)]$^+$ (**3c′***), as was shown by the replacement of the sharp high-field signals in the ^{1}H NMR spectra of the hydrides by broad signals (about −4 ppm) downfield of them that had $T_{1(min)}$ values typical of non-classical dihydrogen compounds [18] (Table 3).

Table 3
Selected NMR data (at 183 K) for the cationic compounds originated by protonation of complexes **3a–c** and **3c′**

Compound[a]	^{1}H NMR;[b] δ (ppm)	Assignment	$T_{1(min)}$ [ms]	^{31}P{^{1}H} NMR; δ (ppm)	T^d (K)
mer-[Re(η^2-H$_2$)(CO)$_3$**L^1**]$^+$ (**3a***)	−4.81 (br)	η^2-H$_2$	14 ± 3 at 197 K	110.0 (br)	263
	2.13 (br)	–CH$_2$–		111.0 (br)	
	3.67–4.12 (br)	–OCH$_2$–			
fac-[Re(η^2-H$_2$)(CO)$_3$**L^2**]$^+$ (**3b***)	−4.47 (br)	η^2-H$_2$	14 ± 3 at 215 K	–[c]	253
	1.16 (br)	–CH$_3$			
	2.47 (br)	–CH<			
	4.05 (br)	–OCH$_2$–			
fac-[Re(η^2-H$_2$)(CO)$_3$**L^3**]$^+$ (**3c***)	−4.43 (br)	η^2-H$_2$	15 ± 2 at 213 K	–[c]	253
	3.80–4.10 (m, br)	–OCH$_2$–			
[{Re(η^2-H$_2$)(CO)$_4$}$_2$(μ-**L^3**)]$^+$ (**3c′***)	−4.16 (br)	η^2-H$_2$	16 ± 3 at 206 K	140.2 (br)	
	4.03 (br)	–OCH$_2$–			243

[a] In CD_2Cl_2 at 400 MHz.
[b] Cyclohexyl and phenyl proton resonances are omitted.
[c] Signal buried in the baseline.
[d] Limit of thermal stability.

These cations, which all had quite similar NMR characteristics (Table 3), released H_2 when the temperature was raised, as was indicated by the appearance of a sharp singlet at 4.6 ppm corresponding to free H_2 [19]. This occurred at lowest temperature for **3c′***, and at highest for **3a*** (Table 3), which may be explained in terms of the number of CO ligands [16] and the nature of the R groups of the phosphinite ligand, as follows. Diphosphinite ligands have lesser π-acceptor properties than carbonyl ligands making the metal centre more electron-rich thus favouring the π back-donation to the H_2 σ* orbital. The amount of π back-donation is crucial: too little backbonding makes the complex unstable towards H_2 release, while too much back-donation converts dihydrogen complexes into classical dihydrido compounds. In the case of dihydrogen complexes **3**(**a**–**c**)* and **3c′*** the back-donation is not enough to produce the homolytic cleavage of the H_2 ligand. Besides, their different stabilities towards H_2 release could be rationalised as a function of the amount of backbonding between the metal centre and the H_2 ligand, being the least stable compound, **3c′***, the only one with four carbonyl groups around the rhenium atom. That compounds **3b*** and **3c*** have similar thermal stabilities may be attributed to their having the same number of carbonyls and similar R groups (isopropyl and cyclohexyl). Compound **3a*** is more stable than **3b***, **3c*** and the similar compound [Re(η^2-H_2)$(CO)_3$L] [L = 1,2-bis(diphenylphosphinoxy)ethane] [7d], which like **3b*** and **3c*** has *fac* stereochemistry and releases hydrogen at about 230 K. The greater stability of **3a*** may be attributed to its dihydrogen ligand being *trans* to a P atom, whereas in the *fac* complexes it is necessarily located *trans* to a CO with greater π-accepting capacity than P.

3. Experimental

All experimental manipulations were carried out under an atmosphere of argon using Schlenk techniques. All the solvents were purified by conventional procedures [20] and distilled prior to use. The ligands 1,2-bis(diisopropylphosphinoxy)ethane (**L²**) and 1,2-bis(dicyclohexylphosphinoxy)ethane (**L³**), and the hydrido precursor [ReH$(CO)_5$], were prepared by published methods [8,21]. ^{1}H, ^{31}P, ^{13}C and ^{19}F NMR spectra were obtained on a Bruker ARX-400 spectrometer operating at frequencies of 400, 161, 100 and 376 MHz, respectively; the spectra were recorded in $CDCl_3$ or CD_2Cl_2 solutions, as indicated, using the solvent as internal lock. ^{1}H and ^{13}C{^{1}H} signals are referred to internal TMS, those of ^{19}F{^{1}H} to $CFCl_3$, and those of ^{31}P{^{1}H} to 85% H_3PO_4; downfield shifts (δ in ppm) are considered positive. IR spectra (KBr discs) were recorded on a Bruker VECTOR IFS 28 FT apparatus, and mass spectra on a Micromass Autospec M LSIMS (FAB$^+$) system. Microanalyses were carried out on a Fisons Model EA 1108 elemental analyzer.

3.1. Synthesis of $Ph_2PO(CH_2)_3OPPh_2$ (**L¹**)

Ph_2PCl (13 mL, 72.4 mmol), Et_3N (10 mL, 72.1 mmol) and toluene (60 mL) were placed into a 250 mL Schlenk flask equipped with an addition funnel in which a solution of 2 mL (36 mmol) of 1,3-propanediol and 35 mL of toluene was placed. This solution was added dropwise at −80 °C and was stirred over 1.5 h. at 0 °C. The solid formed was filtered off, and the solvent and most impurities were removed by distillation under reduced pressure. This gave a viscous oil that was pure enough for NMR analysis but decomposed within 24 h, for which reason this product was kept, and used in subsequent steps, in toluene solution under argon. Yield: 80%. ^{1}H NMR (400 MHz, $CDCl_3$): δ 2.91 (m, 2H, –CH_2–), δ 3.95 (m, 4H, –OCH_2–). ^{31}P{^{1}H} NMR (161 MHz, $CDCl_3$): δ 112.6 (s).

3.2. Preparation of fac-[ReBr$(CO)_3$L] (**1**) [L = **L¹** (**1a**), **L²** (**1b**), **L³** (**1c**)]

[ReBr$(CO)_5$] (0.1 g, 0.25 mmol) was suspended in 10 mL of toluene and an equimolar amount of L was added (1.2 mL of a 0.22 M solution of **L¹**; 0.9 mL of a 0.29 M solution of **L²**; 2.1 mL of a 0.12 M solution of **L³**). The mixture was refluxed for 3–4 h, allowed to cool to room temperature, and stirred for a further 3 h. The solvent was removed under vacuum, and the residue was treated with ethanol (2 mL), affording a white product that was filtered out, washed with ethanol, dried under vacuum, and recrystallized from 2:10 (v/v) CH_2Cl_2/EtOH by slow evaporation.

Compound **1a**. Yield: 56% (0.19 g). *Anal*. Calc. for $C_{30}H_{26}BrO_5P_2Re$: C, 46.0; H, 3.20%. Found: C, 45.35; H, 3.30%. MS (*m*/*z*, referred to the most abundant isotopes): 794, [M]; 766, [M − CO]; 738, [M − 2CO]; 715, [M − Br]. IR(ν_{CO}): 2031, 1948, 1922 cm^{-1}. ^{1}H NMR (400 MHz, $CDCl_3$): δ 1.71–2.32 (m, 2H, –CH_2CH_2–), δ 3.59–4.54 (m, 4H, –OCH_2–), δ 7.32–7.98 (m, 20H, Ph). ^{31}P{^{1}H} NMR (161 MHz, $CDCl_3$): δ 97.7 (s). ^{13}C{^{1}H} NMR (100 MHz, $CDCl_3$): δ 31.8 (s, –CH_2–), δ 66.4 (s, –OCH_2–), δ 128.7–137.2 (m, Ph), δ 188.0 (m, CO *cis* to Br), δ 189.0 (t, $^2J_{CP}$ = 7 Hz, CO *trans* to Br).

Compound **1b**. Yield: 19% (0.07 g). *Anal*. Calc. for $C_{17}H_{32}BrO_5P_2Re$: C, 31.68; H, 5.0%. Found: C, 32.11; H, 5.4%. MS (*m*/*z*, referred to the most abundant isotopes): 644, [M]; 616, [M − CO]; 588, [M − 2CO]; 560, [M − 3CO]. IR(ν_{CO}): 2029, 1951, 1897 cm^{-1}. ^{1}H NMR (400 MHz, $CDCl_3$): δ 1.21–1.38 (m, 24H, –CH_3), δ 2.52–2.95 (m, 4H, ≻CH–), δ 3.83–4.53 (m, 4H, –CH_2CH_2–). ^{31}P{^{1}H} NMR (161 MHz, $CDCl_3$): δ 135.6 (s). ^{13}C{^{1}H} NMR (100 MHz, $CDCl_3$): δ 18.8 (m, –CH_3), δ 29.7 (m, ≻CH–), δ 64.2 (m, –OCH_2CH_2O–), δ 187.9 (t, $^2J_{CP}$ = 8 Hz, CO *trans* to Br), δ 188.2 (m, CO *cis* to Br).

Compound **1c**. Yield: 50% (0.15 g). *Anal*. Calc. for $C_{29}H_{48}BrO_5P_2Re$: C, 43.90; H, 6.40%. Found: C, 43.28; H, 6.01%. MS (*m*/*z*, referred to the most abundant

isotopes): 804, [M]; 748, [M − 2CO]; 720, [M − 3CO]; 725, [M − Br]. IR(ν_{CO}): 2022, 1954, 1888 cm^{-1}. ^1H NMR (400 MHz, $CDCl_3$): δ 1.15–2.55 (m, 44H, Cy), δ 3.84–4.46 (m, 4H, –OCH_2CH_2O–). $^{31}P\{^1H\}$ NMR (161 MHz, $CDCl_3$): δ 129.7 (s). $^{13}C\{^1H\}$ NMR (100 MHz, $CDCl_3$): δ 23.8–28.9(m, C2–C6 of Cy), δ 37.9–43.1 (m, C1 of Cy), δ 64.6 (s, a, –OCH_2), δ 64.9 (s, a, –OCH_2), δ 188.1 (m, CO *cis* to Br), δ 189.0 (t, $^2J_{CP} = 7$ Hz, CO *trans* to Br).

3.3. Preparation of fac-[Re(O_3SCF_3)(CO)$_3$L] (2) [L = L^1 (2a), L^2 (2b), L^3 (2c)]

A mixture of the appropriate compound **1** (0.13 mmol) and $Ag(O_3SCF_3)$ (0.1 mmol) in CH_2Cl_2 (20 mL) was heated under reflux for 1 h and filtered to remove AgBr. The solvent was removed under vacuum, and the residue was treated with ethanol (2 mL), affording a brown product that was filtered out, washed with ethanol and dried under vacuum.

Compound **2a**. Yield: 67% (0.02 g). *Anal.* Calc. for $C_{31}H_{26}F_3O_8P_2ReS$: C, 43.05; H, 3.03%. Found: C, 42.98; H, 2.96%. MS (*m*/*z*, referred to the most abundant isotopes): 864, [M]. IR(ν_{CO}): 2042, 1960, 1940 cm^{-1}. ^1H NMR (400 MHz, $CDCl_3$): δ 1.72–2.16 (m, 2H, –CH_2CH_2–), δ 3.66–3.86 (m, 4H, –OCH_2–), δ 7.19–7.70 (m, 20H, Ph). $^{31}P\{^1H\}$ NMR (161 MHz, $CDCl_3$): δ 112.7 (s). $^{13}C\{^1H\}$ NMR (100 MHz, $CDCl_3$): δ 30.2 (s, –CH_2), δ 64.8 (s, –OCH_2), δ 118.8 (s, –CF_3), δ 128.2–134.9 (m, Ph), δ 189.2 (t, $^2J_{CP} = 7$ Hz, CO *trans* to OTf), δ 189.5 (m, CO *cis* to OTf). $^{19}F\{^1H\}$ NMR (376 MHz, $CDCl_3$): δ −76.9 (s).

Compound **2b**. Yield: 50% (0.02 g). *Anal.* Calc. for $C_{18}H_{32}F_3O_8P_2ReS$: C, 30.25; H, 4.52%. Found: C, 30.22; H, 4.56%. MS (*m*/*z*, referred to the most abundant isotopes): 714, [M]; 658, [M − 2CO]. IR(ν_{CO}): 2038, 1968, 1914 cm^{-1}. ^1H NMR (400 MHz, $CDCl_3$): δ 1.16–1.51 (m, 24H, –CH_3), δ 2.49–2.59 (m, 4H, >CH–), δ 3.98–4.08 (m, 4H, –CH_2CH_2–). $^{31}P\{^1H\}$ NMR (161 MHz, $CDCl_3$): δ 145.0 (s). $^{13}C\{^1H\}$ NMR (100 MHz, $CDCl_3$): δ 16.2 (m, –CH_3), δ 28.1 (m, >CH–), δ 62.1 (m, –OCH_2CH_2O–), δ 118.2 (s, –CF_3), δ 188.9 (t, $^2J_{CP} = 8$ Hz, CO *trans* to OTf), δ 187.2 (m, CO *cis* to OTf). $^{19}F\{^1H\}$ NMR (376 MHz, $CDCl_3$): δ −77.1 (s).

Compound **2c**. Yield: 56% (0.01 g). *Anal.* Calc. for $C_{30}H_{48}F_3O_8P_2ReS$: C, 41.18; H, 5.53%. Found: C, 41.12; H, 5.64%. MS (*m*/*z*, referred to the most abundant isotopes): 874, [M]; 846, [M − CO]; 818, [M − 2CO]; 790, [M − 3CO]. IR(ν_{CO}): 2040, 1972, 1918 cm^{-1}. ^1H NMR (400 MHz, $CDCl_3$): δ 1.16–2.32 (m, 44H, Cy), δ 3.63–4.04 (m, 4H, –OCH_2CH_2O–). $^{31}P\{^1H\}$ NMR (161 MHz, $CDCl_3$): δ 138.8 (s). $^{13}C\{^1H\}$ NMR (100 MHz, $CDCl_3$): δ 26.1–27.4(m, C2–C6 of Cy), δ 40.4–43.2 (m, C1 of Cy), δ 65.9 (s, a, –OCH_2–), δ 118.5 (s, –CF_3), δ 190.2 (m, CO *cis* to OTf), δ 192.1 (t, $^2J_{CP} = 7$ Hz, CO *trans* to OTf). $^{19}F\{^1H\}$ NMR (376 MHz, $CDCl_3$): δ −76.8 (s).

3.4. Preparation of mer-[ReH(CO)$_3$$L^1$] (3a)

A solution of $[ReH(CO)_5]$ (0.1 mL, 0.7 mmol) in THF (10 mL) was added to a solution of $\mathbf{L^1}$ in toluene (10 mL, 0.22 M), the mixture was stirred for 24 h, and the white solid formed was filtered out. This product was a mixture of mer and fac isomers. Washing with THF removed the more soluble *fac*-isomer, leaving the *mer*-isomer, which was washed with 2 mL of ethanol and recrystallized from 2:10 (v/v) CH_2Cl_2/EtOH by slow evaporation. Yield: 39% (0.2 g). *Anal.* Calc. for $C_{30}H_{27}O_5P_2Re$: C, 50.72; H, 3.80%. Found: C, 50.35; H, 3.80%. MS (*m*/*z*, referred to the most abundant isotopes): 716, [M]; 688, [M − CO]. IR(ν_{CO}): 2035, 1954, 1917 cm^{-1}. ^1H NMR (400 MHz, CD_2Cl_2): δ −6.09 (d, 1H, $J_{PH} = 36$ Hz, ReH), δ 2.02 (m, 2H, –CH_2–), δ 3.91 (m, 4H, –OCH_2–), δ 7.50–7.95 (m, 20H, Ph). $^{31}P\{^1H\}$ NMR (161 MHz, CD_2Cl_2): δ 120.8 (d, $J_{PP} = 23$ Hz); 124.4 (d, $J_{PP} = 23$ Hz). $^{13}C\{^1H\}$ NMR (100 MHz, $CDCl_3$): δ 32.7 (t, $^3J_{CP} = 4$ Hz, –CH_2–), δ 59.8 (s, –OCH_2–), δ 61.0 (s, –OCH_2–), δ 127.7–132.5 (m, *ortho*-C, *meta*-C, *para*-C of Ph), δ 141.8 (d, $J_{CP} = 55$ Hz, *ipso*-C of Ph), δ 143.7 (d, $J_{CP} = 49$ Hz, *ipso*-C of Ph), δ 193.2 (t, $J_{CP} = 12$ Hz, *cis* CO), δ 196.9 (m, *trans* CO).

3.5. Preparation of fac-[ReH(CO)$_3$$L^2$] (3b)

A solution of $[ReH(CO)_5]$ (0.1 mL, 0.7 mmol) in THF (10 mL) was added to a solution of [1,2-bis(diisopropylphosphinoxy)ethane] (7.5 mL, 0.29 M) in toluene (Re:L mole ratio 1:3), and the mixture was heated at 60 °C for 6 h. After cooling to room temperature, the solvent was removed under vacuum, and the residual oil was chromatographed on a silica gel column (length 70 cm, diameter 4 cm) using a 10:1 mixture of light petroleum (40–60 °C) and diethyl ether as eluent. The first fraction eluted (25 mL) was concentrated to dryness, leaving an oil that was treated with ethanol (2 mL). Cooling the resulting solution to –25 °C afforded white crystals of complex 3b. Yield: 24% (0.09 g). *Anal.* Calc. for $C_{17}H_{33}O_5P_2Re$: C, 36.10; H, 5.88%. Found: C, 36.40; H, 5.96%. MS (*m*/*z*, referred to the most abundant isotopes): 566, [M]; 538, [M − CO]. IR(ν_{CO}): 2077, 1964, 1914 cm^{-1}. ^1H NMR (400 MHz, CD_2Cl_2): δ −5.69 (t, 1H, $^2J_{HP} = 27$ Hz, ReH), δ 1.04–1.20 (m, 24H, –CH_3), δ 2.16 (m, 2H, >CH–), δ 2.32 (m, 2H, >CH–), δ 4.03 (m, 2H, –OCH_2–), δ 4.23 (m, 2H, –OCH_2–). $^{31}P\{^1H\}$ NMR (161 MHz, CD_2Cl_2): δ 149.5 (s). $^{13}C\{^1H\}$ NMR (100 MHz, $CDCl_3$): δ 17.2, 17.4, 17.8 and 18.6 (all s, CH_3), δ 33.0 (t, $J_{CP} = 15$ Hz, >CH–), δ 33.4 (t, $J_{CP} = 14$ Hz, >CH–), δ 67.0 (m, –OCH_2-CH_2O–), δ 195.6 (m, CO *cis* to H), δ 196.2 (t, $^2J_{CP} = 14$ Hz, CO *trans* to H).

3.6. Preparation of fac-[ReH(CO)$_3$$L^3$] (3c) and [$Re_2H_2(CO)_8$-μ-$L^3$] (3c′)

A solution of $[ReH(CO)_5]$ (0.1 mL, 0.7 mmol) in THF (10 mL) was added to a solution of [1,2-bis(dicyclohexyl-

phosphinoxy)ethane] (17.5 mL, 0.12 M) in toluene, and the reaction mixture was stirred for 5 h. The solvent was removed under reduced pressure, and the residual oil was chromatographed on a silica gel column (length 70 cm, diameter 4 cm) using a 10:1 mixture of light petroleum (40–60 °C) and diethyl ether as eluent. The first fraction eluted (20 mL) was concentrated to dryness, leaving an oil that was treated with ethanol (2 mL). Cooling the resulting solution to −25 °C afforded white crystals of complex **3c′**. Yield of **3c′**: 43% (0.14 g). *Anal*. Calc. for $C_{34}H_{50}O_{10}P_2Re_2$: C, 38.98; H, 4.88%. Found: C, 38.70; H, 4.78%. MS (*m/z*, referred to the most abundant isotopes): 1054, [M]; 1052, [M − 2H]; 1025, [M − CO]; 1023, [M − H − CO]; 998, [M − 2CO]; 997, [M − H − 2CO]; 996, [M − 2H − 2CO]; 968, [M − 2H − 3CO]; 940, [M − 2H − 4CO]. IR(ν_{CO}): 2077, 1991, 1957 cm^{-1}. ^1H NMR (400 MHz, CD_2Cl_2): δ −6.17 (d, 2H, $J_{PH} = 23$ Hz, ReH), δ 1.88–1.22 (m, 44H, Cy), δ 3.93 (m, 4H, –OCH_2-CH_2O–). $^{31}P\{^1H\}$ NMR (161 MHz, CD_2Cl_2): δ 145.9 (s). $^{13}C\{^1H\}$ NMR (100 MHz, $CDCl_3$): δ 22.6–30.0(m, C2–C6 of Cy), δ 44.5 (d, $^1J_{CP} = 30$ Hz, C1 of Cy), δ 72.6 (m, –OCH_2CH_2O–), δ 190.5 (d, $^2J_{CP} = 43$ Hz, *trans* CO–P), δ 192.0 (d, $^2J_{CP} = 10$ Hz, *trans* CO–CO), δ 192.2 (d, $^2J_{CP} = 7$ Hz, *trans* CO–H).

From the second fraction eluted (10 mL), after evaporation of the solvent and treatment with ethanol, a white solid was obtained, complex **3c**.

Yield of **3c**: 10% (0.04 g). *Anal*. Calc. for $C_{29}H_{49}O_5P_2Re$: C, 47.92; H, 6.80%. Found: C, 47.83; H, 6.52%. MS (*m/z*, referred to the most abundant isotopes): 726, [M]; 725, [M − H]; 698, [M − CO]. IR(ν_{CO}): 1998, 1907, 1816 cm^{-1}. ^1H NMR (400 MHz, CD_2Cl_2): δ −5.68 (t, 1H, $J_{PH} = 27$ Hz, ReH), δ 2.05–1.27 (m, 44H, Cy), δ 3.93 (m, 2H, –OCH_2-CH_2O–), δ 4.13 (m, 2H, –OCH_2CH_2O–). $^{31}P\{^1H\}$ NMR (161 MHz, CD_2Cl_2): δ 143.5 (s). $^{13}C\{^1H\}$ NMR (100 MHz, $CDCl_3$): δ 26.3–27.2 (Cy), δ 42.6 (t, $J_{CP} = 14$ Hz, Cy), δ 43.3 (t, $J_{CP} = 14$ Hz, Cy), δ 66.4 (s, –CH_2CH_2–), δ 194.9 (m, *cis* CO–H), δ 196.0 (t, $J_{CP} = 8$ Hz, *trans* CO–H).

3.7. Protonation reactions

Hydrido compounds **3** were protonated following a procedure described in the literature for similar compounds [22].

3.8. X-ray crystallographic analysis

Compounds **1a**–**c**, **3a**, **3b** and **3c′** were mounted on glass fibres and studied on a SIEMENS Smart CCD area-

Table 4
Crystal and structure refinement data for the bromo complexes

Identification code	**1a**	**1b**	**1c**
Empirical formula	$C_{30}H_{26}$ Br O_5P_2 Re	$C_{17}H_{32}$ Br O_5P_2 Re	$C_{29}H_{44}$ Br O_5P_2 Re
Formula weight	794.56	644.48	800.69
T (K)	293(2)	293(2)	293(2)
λ (Å)	0.71073	0.71073	0.71073
Crystal system	Monoclinic	Monoclinic	Triclinic
Space group	$P2_1/n$	$P2_1/n$	$P\bar{1}$
Unit cell dimensions			
a (Å)	11.772(1)	14.517(1)	10.767(1)
b (Å)	15.418(1)	9.911(1)	11.156(1)
c (Å)	16.720(1)	16.563(1)	13.805(1)
α (°)	90	90	89.158(1)
β (°)	91.000(1)	103.438(1)	76.339(1)
γ (°)	90	90	86.639(1)
V (Å^3)	3033.9(3)	2317.8(2)	1608.6(2)
Z	4	4	2
D_{calc} (Mg/m^3)	1.740	1.847	1.653
Absorption coefficient (mm^{-1})	5.464	7.127	5.153
F(000)	1544	1256	796
Crystal size (mm)	0.21 × 0.20 × 0.20	0.47 × 0.44 × 0.17	0.40 × 0.30 × 0.11
θ Range for data collection (°)	1.80–28.00	1.68–28.02	1.52–28.02
Index ranges	$-13 \leqslant h \leqslant 15$, $-19 \leqslant k \leqslant 20$, $-15 \leqslant l \leqslant 22$	$-19 \leqslant h \leqslant 18$, $-13 \leqslant k \leqslant 11$, $-18 \leqslant l \leqslant 21$	$-12 \leqslant h \leqslant 14$, $-14 \leqslant k \leqslant 10$, $-14 \leqslant l \leqslant 18$
Reflections collected	17765	13899	10153
Independent reflections (R_{int})	6922 (0.0439)	5364 (0.0492)	7073 (0.0329)
Reflections observed (>2σ)	4442	4141	6057
Data completeness (%)	94.5	95.7	90.9
Absorption correction	Semi-empirical from equivalents	Semi-empirical from equivalents	Semi-empirical from equivalents
Maximum and minimum transmission	1.000 and 0.667	1.0000 and 0.525267	1.0000 and 0.468384
Data/restraints/parameters	6922/0/352	5364/0/243	7073/0/343
Goodness-of-fit on F^2	0.901	0.970	1.027
Final R indices [$I > 2\sigma(I)$]	$R_1 = 0.0377$, $wR_2 = 0.0816$	$R_1 = 0.0364$, $wR_2 = 0.0842$	$R_1 = 0.0476$, $wR_2 = 0.1285$
R indices (all data)	$R_1 = 0.0751$, $wR_2 = 0.0878$	$R_1 = 0.0528$, $wR_2 = 0.0885$	$R_1 = 0.0551$, $wR_2 = 0.1319$
Largest difference in peak and hole (e Å^{-3})	1.063 and −1.556	2.182 and −1.706	1.893 and −2.967

Table 5
Crystal and structure refinement data for the hydride complexes

Identification code	**3a**	**3b**	**3c′**
Empirical formula	$C_{30}H_{27}O_5P_2$ Re	$C_{17}H_{33}O_5P_2$ Re	$C_{34}H_{46}O_{10}P_2Re_2$
Formula weight	715.66	565.57	1049.05
T (K)	293(2)	293(2)	173(2)
λ (Å)	0.71073	0.71073	0.71073
Crystal system	Monoclinic	Monoclinic	Triclinic
Space group	$P2_1/n$	$P2_1/n$	$P\bar{1}$
Unit cell dimensions			
a (Å)	12.084(1)	14.969(1)	10.029(1)
b (Å)	15.826(1)	9.678(1)	12.268(1)
c (Å)	15.191(1)	16.317(1)Å	16.859(1)
α (°)	90	90	73.497(1)
β (°)	104.295(1)	109.707(1)	83.842(1)
γ (°)	90	90	85.210(1)
V (Å^3)	2815.1(3)	2225.2(2)	1974.3(2)
Z	4	4	2
D_{calc} (Mg/m^3)	1.689	1.688	1.765
Absorption coefficient (mm^{-1})	4.468	5.626	6.257
F(000)	1408	1120	1020
Crystal size (mm)	$0.17 \times 0.16 \times 0.11$	$0.43 \times 0.33 \times 0.15$	$0.40 \times 0.30 \times 0.06$
θ Range for data collection (°)	1.89–28.04	1.60–28.03	1.73–28.03
Index ranges	$-13 \leqslant h \leqslant 15$, $-17 \leqslant k \leqslant 20$, $-19 \leqslant l \leqslant 20$	$-15 \leqslant h \leqslant 19$, $-12 \leqslant k \leqslant 12$, $-21 \leqslant l \leqslant 18$	$-13 \leqslant h \leqslant 13$, $-15 \leqslant k \leqslant 14$, $-21 \leqslant l \leqslant 13$
Reflections collected	16 510	13 383	12 330
Independent reflections (R_{int})	6457 (0.0663)	5159 (0.0495)	8586 (0.0281)
Reflections observed (>2σ)	3751	4011	7142
Data completeness	0.946	0.958	0.897
Absorption correction	Semi-empirical from equivalents	Semi-empirical from equivalents	Semi-empirical from equivalents
Maximum and minimum transmission	1.0000 and 0.7278	1.0000 and 0.4500	1.0000 and 0.6239
Data/restraints/parameters	6457/0/347	5159/0/238	8586/0/441
Goodness-of-fit on F^2	0.802	0.947	1.003
Final R indices [$I > 2\sigma(I)$]	$R_1 = 0.0416$, $wR_2 = 0.0526$	$R_1 = 0.0347$, $wR_2 = 0.0755$	$R_1 = 0.0346$, $wR_2 = 0.0806$
R indices (all data)	$R_1 = 0.0955$, $wR_2 = 0.0591$	$R_1 = 0.0492$, $wR_2 = 0.0789$	$R_1 = 0.0444$, $wR_2 = 0.0845$
Largest difference in peak and hole (e Å^{-3})	1.626 and −1.427	2.076 and −1.849	1.850 and −1.882

detector diffractometer using graphite-monochromated Mo Kα radiation ($\lambda = 0.71073$ Å). The crystal parameters and experimental details of data collection are summarized in Tables 4 and 5. ORTEP [23] drawings of the compounds, along with the numbering schemes adopted, are shown in Figs. 1, 2, 3 and 7, 8, 9. Absorption corrections were carried out using SADABS [24]. All the structures were solved by direct methods except **3c′**, which was solved by the Patterson method. All structures were refined by full-matrix least-squares based on F^2 [25]. All non-hydrogen atoms were refined with anisotropic displacement parameters. All hydrogen atoms were refined with isotropic displacement parameters following location in a difference electron density map (in the case of the hydride atoms) or inclusion at idealized positions (all others). Atomic scattering factors and anomalous dispersion corrections for all atoms were taken from International Tables for X-ray Crystallography [26].

4. Conclusions

A new diphosphinite ligand, 1,3-bis(diphenylphosphinoxy)propane (**L^1**), the bromo complexes *fac*-[ReBr(CO)$_3$-**L$^{1-3}$**] [**1a**–**c**; **L^2** = 1,2-bis(diisopropylphosphinoxy)ethane, **L^3** = 1,2-bis(dicyclohexylphosphinoxy)ethane], the triflato complexes *fac*-[Re(OTf)(CO)$_3$**L$^{1-3}$**] (**2a**–**c**) and the hydrido complexes *mer*-[ReH(CO)$_3$**L^1**] (**3a**), *fac*-[ReH(CO)$_3$**L^{2,3}**] (**3b**,**3c**) and [{ReH(CO)$_4$}$_2$(μ-**L^3**)] (**3c′**) have been synthesized and characterized. The bromo and triflato derivatives are all mononuclear compounds with *fac*-CO groups. However, the nuclearity and stereochemistry of the hydrido compounds depend on the diphosphinite ligand. Surprisingly, no dinuclear complex of **L^1** was obtained, even though its longer between-P spacer was expected to favour its acting as a bridging ligand. The influence of the co-ligands emerged mainly in their effects on the stability of the cationic dihydrogen compounds obtained upon protonation of the hydride complexes: complexes **3**(**a**–**c**)* and **3c′*** are all thermally unstable towards H_2 release and homolytic cleavage of the H_2 ligand was not observed; compound **3a***, the only one in which the η^2-H_2 ligand is *trans* to a diphosphinite P atom, is the most stable; **3b***,**3c*** and *fac*-[Re(η^2-H_2)(CO)$_3$(L)] [L = 1,2-bis(diphenylphosphinoxy)ethane] [7d], which all have similar geometry, have thermal stabilities that correlate well with the electronegativity of the R groups of the diphosphinite ligand; and compound **3c′*** is the least stable, probably because of its 4:1 carbonyl:phosphorus ratio [16], reducing

the backbonding between the metal centre and the H_2 ligand.

5. Supplementary material

Crystallographic data have been deposited with the Cambridge Crystallographic Data Centre, CCDC Nos. 265545–265550. Copies of this information may be obtained free of charge from the CCDC, 12 Union Road, Cambridge CB2 1EZ, UK (fax: +44 1223 336 003; e-mail: deposit@ccdc.cam.ac.uk or www: http://www.ccdc.cam.ac.uk).

Acknowledgements

Financial support from the Xunta de Galicia (Project PGIDT04PXIC31401PN) and the Spanish Ministry of Education (Project BQU2003-06783) is gratefully acknowledged. We thank the University of Vigo CACTI services for collecting X-ray data and recording NMR spectra.

References

[1] M.A. Esteruelas, A.M. Lopez, in: M. Peruzzini, R. Poli (Eds.), Recent Advances in Hydride Chemistry, Elsevier, Amsterdam, 2001 (Chapter 7).
[2] A.J. Maeland, in: M. Peruzzini, R. Poli (Eds.), Recent Advances in Hydride Chemistry, Elsevier, Amsterdam, 2001 (Chapter 18).
[3] P.W.N.M. van Leeuwen, in: Homogeneous Catalysis: Understanding the Art, Kluwer Academic Publishers, Dordrecht, 2004.
[4] J.M. O'Connor, in: E.W. Abel, F.G.A. Stone, G. Wilkinson (Eds.), Comprehensive Organometallic Chemistry II, vol. 6, Pergamon Press, Oxford, 1995 (Chapter 9).
[5] U. Abram, in: J.A. McCleverty, T.J. Meyer (Eds.), Comprehensive Coordination Chemistry II, vol. 5, Elsevier, Amsterdam, 2004 (Chapter 3).
[6] C.A. Tolman, Chem. Rev. 77 (1977) 313.
[7] (a) S. Bolaño, J. Bravo, S. Garcia-Fontan, Eur. J. Inorg. Chem. (2004) 4812;
(b) S. Bolaño, J. Bravo, S. Garcia-Fontan, J. Castro, J. Organometal. Chem. 667 (2003) 103;
(c) S. Bolaño, J. Bravo, S. Garcia-Fontan, Inorg. Chim. Acta 315 (2001) 81;
(d) S. Bolaño, J. Bravo, R. Carballo, S. Garcia-Fontan, U. Abram, E.M. Vazquez-Lopez, Polyhedron 18 (1999) 1431.
[8] L.C. Baldwin, M.J. Fink, J. Organomet. Chem. 646 (2002) 230.
[9] L.H. Staal, A. Oskam, K. Vrieze, J. Organomet. Chem. 170 (1979) 235.
[10] (a) See, for example: J. Zhang, J.J. Vittal, W. Henderson, J.R. Wheaton, I.H. Hall, T.S.A. Hor, Y.K. Yan, J. Organomet. Chem. 650 (2002) 123;
(b) M.S. Balakrishna, M.G. Walawalker, J. Organomet. Chem. 628 (2001) 76;
(c) R. Schibli, K.V. Katti, W.A. Volkert, C.L. Barnes, Inorg. Chem. 40 (2001) 2358.
[11] D.H. Gibson, H. He, M.S. Mashuta, Organometallics 20 (2001) 1456.
[12] The reaction was carried out at 60 °C because at room temperature the yield was very low, as shown by NMR $^{31}P\{^1H\}$ spectrum of the crude mixture.
[13] H. Günther, in: NMR Spectroscopy: Basic Principles, Concepts, and Applications in Chemistry, Wiley, Chichester, 1995.
[14] The interconversion barrier between the chair and boat families of cycloheptane has been computed to be about 33 kJ/mol U. Burkert, N.L. Allinger, Molecular Mechanics, ACS Monograph 177, American Chemical Society, Washington, DC, 1982.
[15] P.J. Desrosiers, L. Cai, Z. Lin, R. Richards, J. Halpern, J. Am. Chem. Soc. 113 (1991) 4173.
[16] G. Albertin, S. Antoniutti, S. Garcia-Fontan, R. Carballo, F. Padoan, J. Chem. Soc., Dalton Trans. (1998) 2071.
[17] C. Bianchini, A. Marchi, L. Marvelli, M. Peruzzini, A. Romerosa, R. Rossi, A. Vacca, Organometallics 14 (1995) 3203.
[18] D.G. Hamilton, R.H. Crabtree, J. Am. Chem. Soc. 110 (1988) 4126.
[19] M.T. Costello, P.E. Fanwick, M.A. Green, R.A. Walton, Inorg. Chem. 31 (1992) 2359.
[20] D.D. Perrin, W.L.F. Armarego, third ed.Purification of Laboratory Chemicals, Butterworth/Heinemann, London/Oxford, 1988.
[21] M.A. Urbanic, J.R. Shapley, Inorg. Synth. 28 (1990) 165.
[22] S. Garcia-Fontan, A. Marchi, L. Marvelli, R. Rossi, S. Antoniutti, G. Albertin, J. Chem. Soc., Dalton Trans. (1996) 2779.
[23] L.J. Farrugia, J. Appl. Crystallogr. 30 (1997) 565.
[24] G.M. Sheldrick, SADABS: An Empirical Absorption Correction Program for Area Detector Data, University of Göttingen, Göttingen, Germany, 1996.
[25] G.M. Sheldrick, SHELX-97: Program for the Solution and Refinement of Crystal Structures, University of Göttingen, Göttingen, Germany, 1997.
[26] A.J.C. Wilson (Ed.), International Tables for Crystallography, vol. C, Kluwer Academic Publishers, Dordrecht, 1992.